LETTERS
PUBLISHED ONLINE: 18 DECEMBER 2011 | DOI: 10.1038/NNANO.2011.223
nature nanotechnology

Intracellular recordings of action potentials by an extracellular nanoscale field-effect transistor

Xiaojie Duan[1], Ruixuan Gao[1], Ping Xie[1], Tzahi Cohen-Karni[2], Quan Qing[1], Hwan Sung Choe[3], Bozhi Tian[1], Xiaocheng Jiang[1] and Charles M. Lieber[1,2]*

The ability to make electrical measurements inside cells has led to many important advances in electrophysiology[1–6]. The patch clamp technique, in which a glass micropipette filled with electrolyte is inserted into a cell, offers both high signal-to-noise ratio and temporal resolution[1,2]. Ideally, the micropipette should be as small as possible to increase the spatial resolution and reduce the invasiveness of the measurement, but the overall performance of the technique depends on the impedance of the interface between the micropipette and the cell interior[1,2], which limits how small the micropipette can be. Techniques that involve inserting metal or carbon microelectrodes into cells are subject to similar constraints[4,7–9]. Field-effect transistors (FETs) can also record electric potentials inside cells[10], and because their performance does not depend on impedance[11,12], they can be made much smaller than micropipettes and microelectrodes. Moreover, FET arrays are better suited for multiplexed measurements. Previously, we have demonstrated FET-based intracellular recording with kinked nanowire structures[10], but the kink configuration and device design places limits on the probe size and the potential for multiplexing. Here, we report a new approach in which a SiO_2 nanotube is synthetically integrated on top of a nanoscale FET. This nanotube penetrates the cell membrane, bringing the cell cytosol into contact with the FET, which is then able to record the intracellular transmembrane potential. Simulations show that the bandwidth of this branched intracellular nanotube FET (BIT-FET) is high enough for it to record fast action potentials even when the nanotube diameter is decreased to 3 nm, a length scale well below that accessible with other methods[1,2,4]. Studies of cardiomyocyte cells demonstrate that when phospholipid-modified BIT-FETs are brought close to cells, the nanotubes can spontaneously penetrate the cell membrane to allow the full-amplitude intracellular action potential to be recorded, thus showing that a stable and tight seal forms between the nanotube and cell membrane. We also show that multiple BIT-FETs can record multiplexed intracellular signals from both single cells and networks of cells.

Our BIT-FET (Fig. 1a) is a combination of a silicon nanowire FET detector and an electrically insulating SiO_2 nanotube that connects the FET to the intracellular fluid (the cytosol). When there is a change in transmembrane potential V_m, such as during an action potential, the varying potential of the cytosol inside the nanotube gives rise to a change in the conductance G of the FET in a manner equivalent to applying a time-varying potential to the gate electrode in a traditional FET. For a p-type FET under constant source/drain (S/D) bias the polarity of the change in G is inverted with respect to that in V_m (Fig. 1a). This BIT-FET design uses the tip of a size-controllable nanotube to interface with cells, which represents the smallest ultimate probe size (enabled by the use of the FET sensor). Because the nanotube is built on top of the planar FET, BIT-FET arrays can fully take advantage of the high density of planar nanoFETs, in contrast to previous work[10].

The BIT-FET devices were prepared through a sequence of growth and fabrication steps that enable control of key individual device parameters as well as the density of multiple devices (Supplementary Fig. S1). Germanium nanowire branches grown on top of silicon nanowires using a gold-nanocluster-catalysed vapour–liquid–solid mechanism[13] were used as sacrificial templates for the nanotubes (see Supplementary Information). Representative scanning electron microscopy (SEM) images show a gold nanodot and the resulting germanium nanowire branch 'standing up' on the silicon nanowire and oriented nearly normal to the substrate surface (Fig. 1b). After defining S/D contacts on each side of selected germanium nanowires (Supplementary Fig. S1d), a conformal, controlled-thickness SiO_2 layer deposited by atomic layer deposition (ALD)[14] provided the nanotube wall and S/D passivation (see Supplementary Information). Representative SEM images of the resulting structure clearly show this conformal SiO_2 shell and the germanium core (Fig. 1c; Supplementary Fig. S2).

Fabrication of the BIT-FET devices was completed by two etching steps (Supplementary Fig. S1). In the first, the topmost part of the SiO_2 shell was selectively removed with buffered hydrofluoric acid to expose the germanium core; in the second, the germanium nanowire was etched away to leave a hollow SiO_2 nanotube on a silicon nanowire. SEM images confirm that the end of the nanotube is open (Fig. 1d). Comparison of images before and after etching further shows that the nanotube structure is open to the silicon nanowire surface, as indicated by the bright to dark change in image contrast associated with removal of the germanium (Fig. 1, Supplementary Fig. S2). These images also demonstrate that the SiO_2 shell is tapered at the tip; for the 50-nm-diameter germanium nanowire and 50-nm-thick ALD SiO_2 used here, the very tip of the nanotube has an outer diameter of ~55 nm, which increases to a maximum of 150 nm at a distance of ~2.2 μm from the tip. This tapering effect results from isotropic etching by the buffered hydrofluoric acid (see Supplementary Information), and we believe this is a particularly advantageous feature in that it leads to a decrease in probe size.

We characterized the electrical properties of the BIT-FETs and several control devices in solution to elucidate the behaviour of this new device architecture. The SEM image in Fig. 2a shows a representative two-FET structure, where a BIT-FET and a conventional FET with similar channel length were fabricated with a

[1]Department of Chemistry and Chemical Biology, Harvard University, Cambridge, Massachusetts, 02138, USA, [2]School of Engineering and Applied Sciences, Harvard University, Cambridge, Massachusetts, 02138, USA, [3]Department of Physics, Harvard University, Cambridge, Massachusetts, 02138, USA. *e-mail: cml@cmliris.harvard.edu

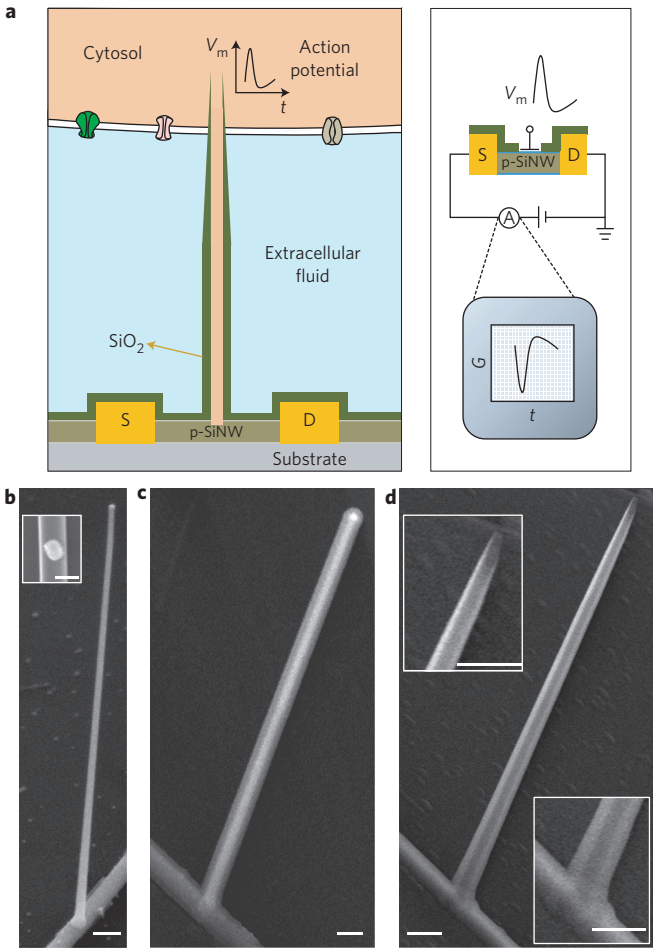

Figure 1 | Branched intracellular nanotube field-effect transistor (BIT-FET). **a**, Schematic diagrams showing (left) a cell coupled to a BIT-FET and the variation in device conductance *G* (right) with time *t* during an action potential V_m. S and D indicate source and drain electrodes. The SiO_2 nanotube connects the cytosol (orange) to the p-type silicon nanowire FET and, together with the SiO_2 passivation (green), excludes the extracellular medium (light blue) from the active device channel. The structures on the membrane represent different ion channels, and are not scaled to the true size of the BIT-FET. **b**, SEM image of a germanium nanowire branch on a silicon nanowire oriented close to the surface normal. Inset: gold nanodot on a silicon nanowire before growth of the germanium nanowire. **c**, SEM image of a germanium/silicon heterostructure coated with ALD SiO_2. Magnified images of the top and bottom are shown in Supplementary Fig. S2. **d**, SEM image of a final nanotube on a silicon nanowire. Insets: magnified images of the top and bottom of the nanotube. Scale bars: 100 nm (inset of **b**), 200 nm (all other images).

common S electrode on the same silicon nanowire. In both devices, the silicon nanowire and electrodes exposed to solution were passivated with ~50 nm ALD SiO_2 as described above. Before etching the germanium core of the BIT-FET, measurements of *G* for both devices as a function of water-gate voltage (V_{wg}) (Fig. 2b) show very little variation (with a sensitivity of approximately -170 nS V^{-1}). Significantly, measurements made on the same devices after removal of the germanium nanowire core (to yield an open nanotube structure; Fig. 2c, inset) demonstrate a large increase in the sensitivity of the BIT-FET to $-4{,}530$ nS V^{-1}, whereas the control FET shows no change (Fig. 2c). Taken together, these results confirm that BIT-FET devices respond selectively and with high sensitivity to the solution inside the nanotubes rather than that outside, and thus meet the requirements for intracellular recording outlined schematically in Fig. 1a. The difference in sensitivity of the BIT-FET devices to solution inside rather than outside the nanotubes originates primarily from the gate capacitance difference[11,12]. Specifically, germanium over-coating on the silicon nanowire may lead to a larger contact area between the silicon nanowire and the internal solution of the nanotube (the active FET area) than defined by the nanotube inner diameter, which can increase this difference in sensitivity (see Supplementary Information).

We also characterized the temporal response of BIT-FET devices to assess their ability to record fast cellular processes. Accordingly, a pulsed V_{wg} with a rise/fall time of 0.1 ms, duration of 1 ms and amplitude of 100 mV was applied to approximate an action potential. The conductance exhibited a peak (dip) coincident with the 0.1 ms rise (fall) of the pulse, and a plateau step down during the constant 100 mV portion of the pulse (Fig. 2d). With rise/fall times ranging from 0.1 to 50 ms for the pulsed V_{wg}, the conductance change associated with the baseline to plateau was found to be independent of the pulse rise time (Fig. 2e); this change is consistent with the device sensitivity determined from quasi-static measurements (for example, Fig. 2c).

The peak and dip features in the pulsed V_{wg} results correspond to the expected capacitive charging[15] of the passivated metal electrodes and are not intrinsic to the BIT-FET. Specifically, a control pulsed V_{wg} measurement made on a silicon-nanowire FET without a nanotube branch showed the same peak (dip) features associated with the rapid rise (fall) of the V_{wg} pulse (Supplementary Fig. S4a). These capacitive features can be readily removed from the BIT-FET and control device data to yield the pure FET response (red curves, Fig. 2d and Supplementary Fig. S4a; in the case of the BIT-FET, this demonstrates clearly that the conductance change follows the 0.1 ms V_{wg} pulse rise/fall without detectable delay. The results shown in Fig. 2d,e demonstrate that the BIT-FET can faithfully record potential changes with a time resolution of at least 0.1 ms. Indeed, our modelling (below) indicates that the temporal resolution, which is beyond our measurement capabilities, should be much better than this value. We also note that these capacitive features would not be expected in cellular measurements because (i) the metal electrodes are only coupled to extracellular media, where the potential changes are quite small[16], and (ii) these changes will be localized on the size scale of a cell, which is much smaller than the electrode area exposed to solution ($\sim cm^2$) in the pulsed V_{wg} experiments here.

We also modelled the BIT-FET device to estimate the bandwidth (which is beyond our current measurement limit) and its dependence on nanotube diameter. The signal transduction in the BIT-FET device can be readily solved by the classical transmission line model[15]. In our analysis (see Supplementary Information), we determined the change in potential at the silicon-nanowire FET surface (V_n) as a function of time following a step change in the transmembrane potential at the nanotube opening to V_0. For a typical nanotube (inner diameter, 50 nm; ALD SiO_2 thickness, 50 nm; length, 1.5 μm), the calculated response (inset, Fig. 2f) yields a bandwidth of ~1.2 MHz. This represents an upper limit assuming that the active FET area and relevant device capacitance C_{NW} (Supplementary Fig. S4b) are defined only by the nanotube inner diameter, and could be reduced to 0.2 MHz if we assume the entire silicon nanowire surface is active due to germanium over-coating. A summary of the results (Fig. 2f) shows that the BIT-FET can achieve a bandwidth of ≥6 kHz (which is sufficient for recording a rapid neuronal action potential[1,2]) for nanotube inner diameters as small as 3 nm (fixed length, 1.5 μm). The high bandwidth determined for the BIT-FET devices results in large part from the small device capacitance, despite the increasingly large solution resistance within the nanotube with decreasing inner diameter (see Supplementary Information). The small diameters accessible with the BIT-FET suggest that it could be minimally

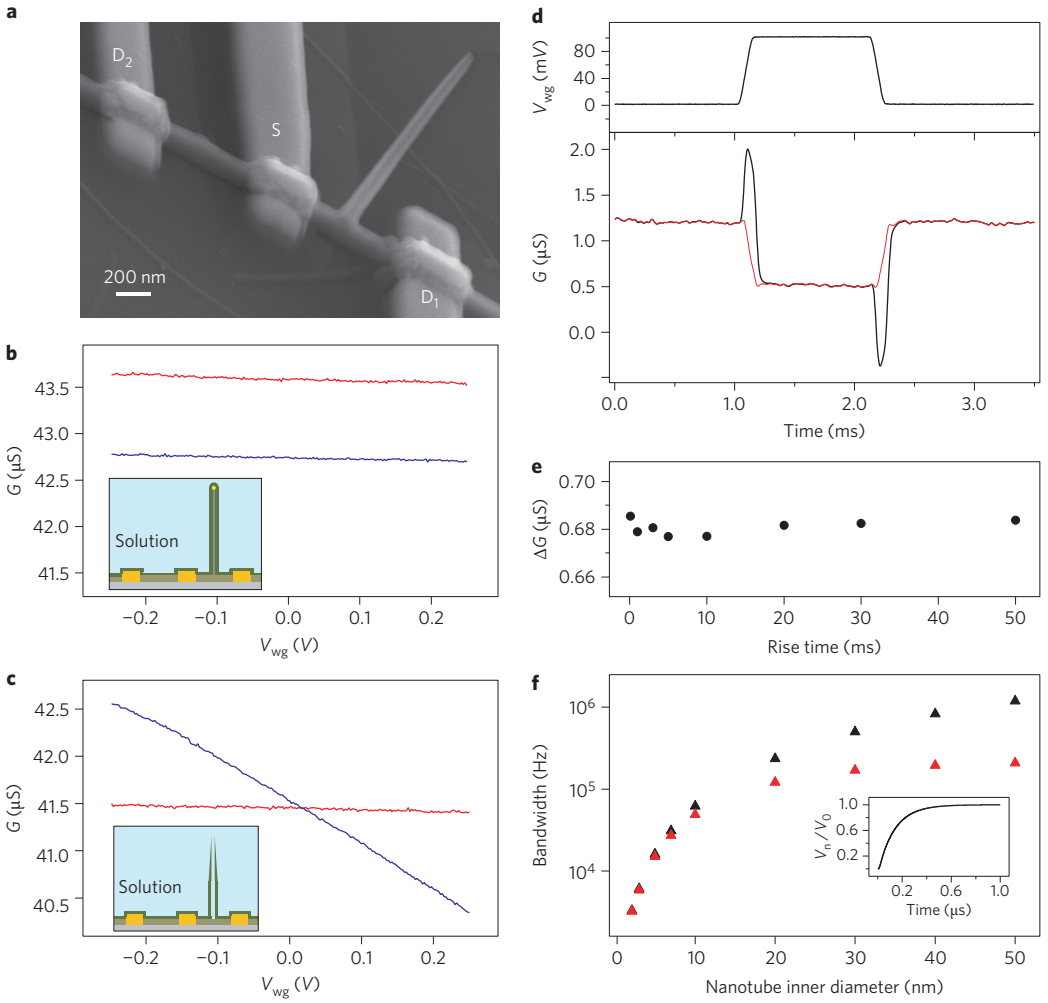

Figure 2 | Water gate characterization and bandwidth analysis. a, SEM image of a BIT-FET device (S–D_1) and control device (S–D_2). **b**,**c**, Conductance G versus water-gate voltage V_{wg} before (**b**) and after (**c**) etching of the germanium nanowire for the BIT-FET (blue) and control device (red). **d**, A V_{wg} pulse (top) with an amplitude of 100 mV and duration of 1 ms (rise and fall times of 0.1 ms), and the corresponding plot of conductance versus time for a BIT-FET device (black trace, bottom). The red trace is the pure field-effect response after removing the capacitive signals of the passivated metal electrodes (see Supplementary Information). **e**, Change in conductance (measured between baseline and plateau) versus the rise/fall time of the V_{wg} pulse for the BIT-FET device studied in **d**. The change was measured as an average over data 0.2–0.5 ms after the start of the pulse. The pulse amplitude was kept at 100 mV, and the duration was ten times the rise/fall time in all measurements. **f**, Calculated bandwidth of the BIT-FET device versus the inner diameter of the nanotube (ALD SiO_2 thickness was the same as the nanotube inner diameter, and the nanotube length was fixed at 1.5 μm). Black and red symbols correspond to upper and lower limits, respectively (see Supplementary Information). Inset: calculated value of V_n/V_0 versus time, where V_n is the potential at the surface of the silicon nanowire FET, and V_0 is the step change in potential at the nanotube opening.

invasive and capable of probing the smallest cellular structures, including neuron dendrites and dendritic spines, which is difficult using conventional electrical-based techniques[17,18].

We investigated the capability of the BIT-FET to record intracellular signals using spontaneously beating embryonic chicken cardiomyocyte cells, which were cultured on thin pieces of polydimethylsiloxane (PDMS) as described previously[16]. After modifying the devices with phospholipids[10] to facilitate the internalization of the nanotubes into cells, the PDMS–cell sheet was manipulated to put a cell into gentle contact with the nanotube of a BIT-FET under a standard electrophysiology microscope (see Supplementary Information). Approximately 45 s after gentle contact was made and in the absence of an applied force on the cell substrate, the recorded data showed a dramatic change (Fig. 3a). Before the transition to intracellular signal, the signal exhibits a relatively flat baseline with small biphasic peaks (amplitude, ~5–8 mV; duration, ~1 ms) with a frequency of ~1 Hz (Fig. 3b,c). These peaks are coincident with cell beating and consistent with extracellular recording reported previously[16]. The baseline then shifts approximately −35 mV, and new peaks with an amplitude of 75–100 mV and duration of ~200 ms are observed (Fig. 3a). The recorded conductance data give inverted peaks for the p-type silicon nanowire FETs used here, although the calibrated potentials are consistent with standard peak polarity and the shape of intracellular action potentials. These peaks (Fig. 3d) have the shape and features characteristic of the intracellular action potential of cardiomyocyte cells[10,19,20], including fast depolarization at the beginning of the peak, a plateau region, fast repolarization and hyperpolarization, and a return to baseline. The signal transition from extra- to intracellular indicates penetration of the cell by the nanotube. The baseline shift is similar to that measured recently using kinked-nanowire probes[10], but smaller than the standard resting potential for cardiomyocytes[19,20]. Our reproducible and stable recording of full-amplitude action potentials, which is a central result of our work, suggests that this baseline difference is not due to poor sealing during nanotube internalization. We

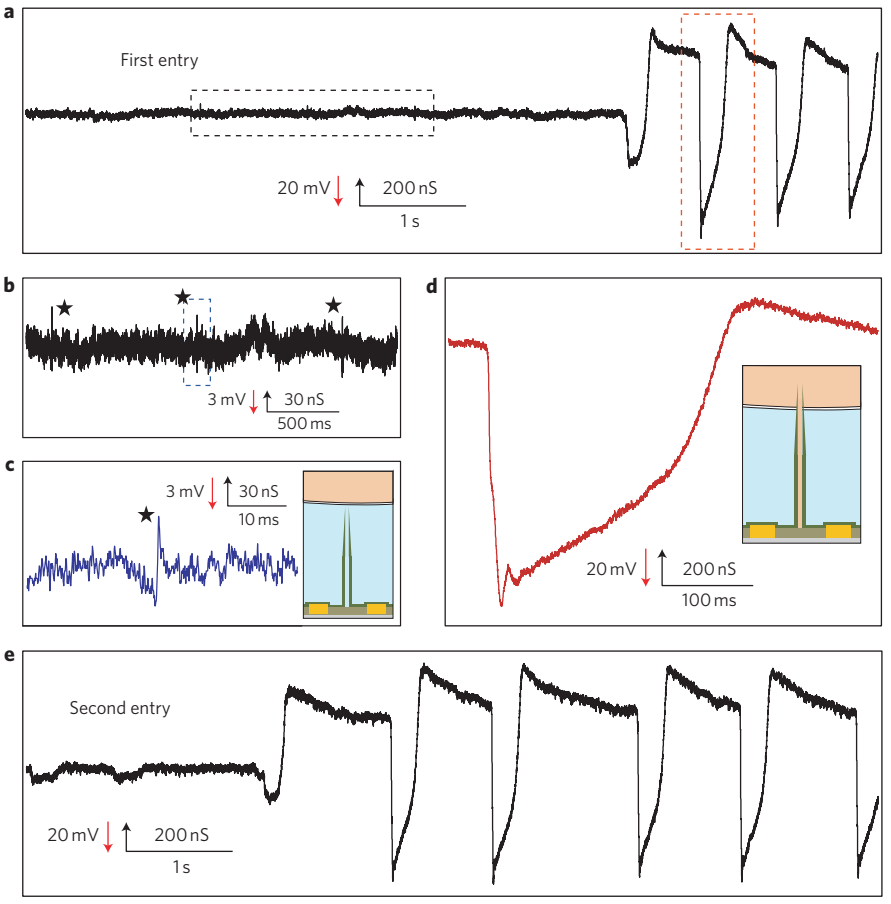

Figure 3 | Recording intracellular action potentials. a, Representative trace (conductance versus time) reflecting the transition from extracellular to intracellular recording. **b**, Magnified view of the trace inside the black dashed rectangle in **a. c**, Magnified view of the trace inside the blue dashed rectangle in **b**. The stars in **b** and **c** mark the position of extracellular spikes. **d**, Magnified view of the peak inside the red dashed rectangle in **a. e**, Trace corresponding to the second entry of the nanotube around the same position on the cell. The potential was calibrated using the sensitivity values measured on phospholipid-modified devices by quasi-static V_{wg} measurement (like the blue trace in Fig. 2c) and pulsed V_{wg} measurement with a rise/fall time of 0.1 ms (same for Fig. 4). The sensitivity obtained from these two measurements is the same as discussed before.

propose that the discrepancy in the resting potentials could be attributed to a stronger suspension effect introduced by the intracellular polyelectrolytes at the junction[21,22] owing to the order-of-magnitude smaller size of the SiO_2 nanotube opening than in a typical patch-clamp pipette. More detailed studies will be required to quantitatively understand the origin of this effect. Although the nanotube dimensions routinely used in our intracellular recording studies (inner diameter, 50 nm; tip outer diameter, 55 nm) are larger than the smallest achievable for BIT-FETs (Fig. 2f), they are still much smaller than the typical glass micropipettes[1,2] and metal microelectrodes[3,4,7] used in intracellular studies.

The change from the extracellular signal to intracellular signal without applying external force to the cell suggests the spontaneous penetration of the cell membrane by the nanotube rather than mechanical insertion. We speculate that lipid fusion[23,24] may play an important role in this penetration, similar to our previous observations[10], and that the small nanotube size is probably beneficial both for this lipid fusion process and for the formation of a tight seal. There are several attractive consequences arising from this spontaneous penetration. First, it typically leads to full-amplitude recording of the action potential (Fig. 3), without the need for circuitry to compensate for probe–membrane leakage, thus suggesting tight sealing between the nanotube and cell membrane. Indeed, control experiments carried out without phospholipid modification of the BIT-FETs required external forces to achieve the transition to intracellular action potential signals, and the smaller amplitude of these signals (10–30 mV) suggests leakage at the nanotube–membrane interface[3]. Second, we find that spontaneous penetration occurs in the same way for a broad range of nanotube orientations (that is, within 30° of the surface normal), in contrast to mechanical insertion. Third, we believe that the tight nanotube–membrane seal and the very small nanotube internal volume, ~3 al, help to preserve cell viability and a stable signal over time. In general, we find that the termination of signal recording by the BIT-FET is due to random separation of the nanotube as a result of the motion of the beating cardiomyocyte cell, and not to cell death or degradation of the nanotube/cell membrane interface (the latter is normally the case when recording with glass micropipettes[1,2]). In addition, and unlike a glass micropipette, when the BIT-FET nanotube is separated from a cell (on purpose, as shown in the following, or as a result of the beating motion), the nanotube can re-penetrate the same cell multiple times at approximately the same position without affecting the cell or the recorded signal. Finally, the total recording time from multiple penetrations with the BIT-FET at a given position on a cell can exceed an hour.

The BIT-FET devices are also robust and reusable. Specifically, following retraction of the cell substrate from the device, which results in the conductance returning to the extracellular baseline, subsequent gentle contact of the nanotube to the same cell without

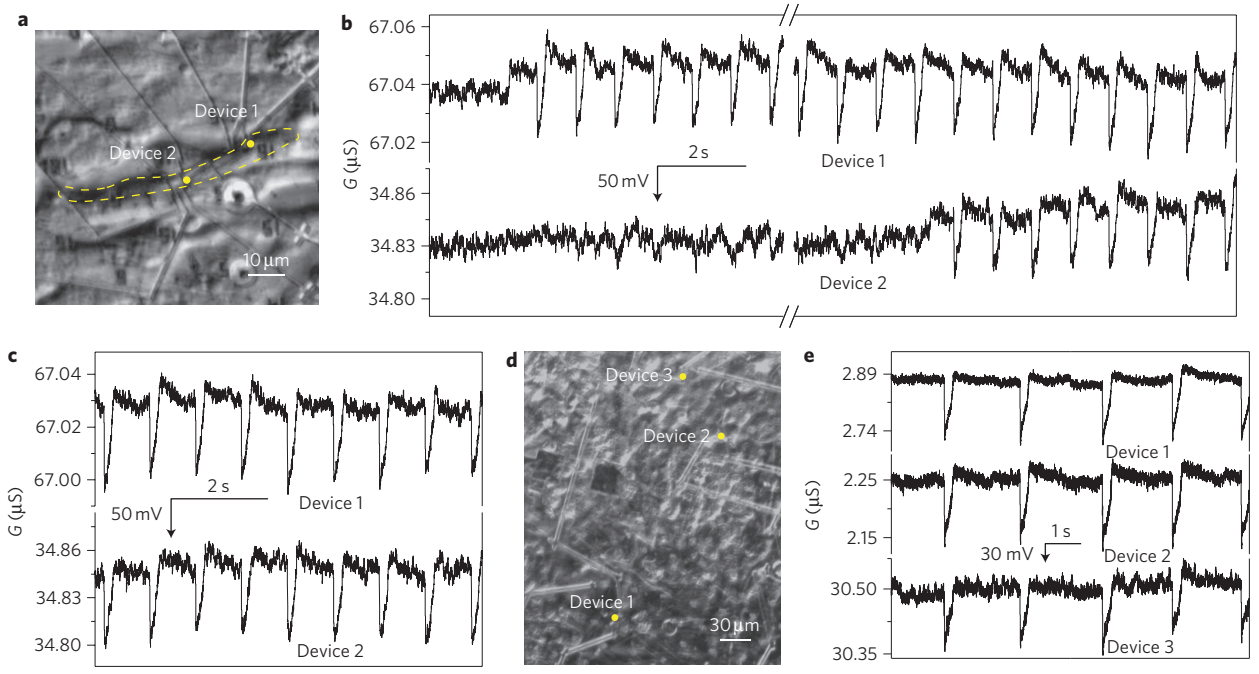

Figure 4 | Multiplexed intracellular recording. a, Differential interference contrast (DIC) microscopy image of two BIT-FET devices (positions marked with dots) coupled to a single cardiomyocyte cell, with the cell boundary marked by the yellow dashed line. **b**, Simultaneously recorded traces from the two devices in **a**, corresponding to the transition from extracellular to intracellular recording. The transition happened in a sequential manner. The break mark labels the ~1 s discontinuity between the two adjacent traces. **c**, Representative trace of stable intracellular action potentials recorded ~120 s after internalization of the devices in **a. d**, DIC image of three BIT-FET devices coupled to a beating cardiomyocyte cell network (from a different PDMS–cell sample). **e**, Representative traces recorded simultaneously from the devices shown in **d**. The three devices measure intracellular action potential signals from different cells in the cell network. Note that the devices used in **a** and **d** have different sensitivities (and are also different from the one used in Fig. 3). These differences are due to variations in the silicon nanowires, FET channel length and growth conditions for the germanium nanowires (see Supplementary Information). The potential was calibrated using the sensitivity values measured for each individual device, and all devices yield corresponding intracellular action potential values with a full amplitude of 75–100 mV (independent of this conductance and sensitivity variation).

changing position leads once again to the development of stable intracellular action potential signals (Fig. 3e). We have repeated the gentle contact/intracellular recording/retraction cycle up to five times with the same BIT-FET nanotube near the same position on the cell without any observable change in the beating frequency and action potential features. A SEM image of the BIT-FET device following these repeated cycles (Supplementary Fig. S5) shows that the nanotube remains intact with some residue on the upper outer surface. In addition, we did not see evidence of blockage of the nanotube during these cycles, which we attribute to the spontaneous penetration mechanism rather than suction or mechanical insertion. Note that the devices can even be reused after being dried. Taken together, these results demonstrate the reliability and robustness of the BIT-FETs and strongly suggest that this is a minimally invasive intracellular recording technique.

A feature of our BIT-FET design is its facility for the straightforward fabrication of multiple, independent devices to enable multiplexed recording from single cells and cell networks. For example, we have readily aligned two phospholipid-modified BIT-FET devices, separated by ~20 µm, with a single, beating cardiomyocyte cell (Fig. 4a). Following gentle contact, conductance versus time measurements made simultaneously using both devices (Fig. 4b) show that device 1 first bridged the cell membrane to yield clear intracellular signals. Approximately 10 s later, we observed the development of intracellular peaks from device 2. Subsequently, intracellular signals were recorded from both devices (Fig. 4c). We can glean several important points from these data. First, the sequential nature with which the intracellular signals develop, in the absence of an applied force, strongly supports the suggestion above that penetration of the cell membrane by the phospholipid-modified nanotubes is a spontaneous biomimetic process that does not adversely affect the cell. Second, the intracellular peaks recorded simultaneously by devices 1 and 2 (full amplitude, 75–100 mV) and stable cell beating over time are consistent with a tight seal being established between the cell membrane and the nanotubes in both devices. In addition, we have also demonstrated that multiplexed measurements with BIT-FETs can be extended to cell networks (Fig. 4d,e). We have recorded intracellular action potentials simultaneously from different sites in a monolayer of beating cardiomyocyte cells. In the future, we suggest that this BIT-FET design will be implementable on high-density integrated planar nanoFETs, either large arrays of nanowire FETs[25] or conventional top-down nanoFET arrays[26], to enable multiplexed recording at a far higher density than demonstrated in these initial studies.

Additional work remains to be done to improve further the BIT-FET-based intracellular measurement technique. The signal-to-noise ratio is still lower than that of glass micropipettes. Implementing the capability for cell stimulation in addition to recording will also be important for intracellular studies. However, we believe that the advantages of the BIT-FET already demonstrated in this work, including the capability to realize sub-5 nm probes, the formation of tight nanotube–cell membrane seals and the potential for large-scale, high-density, multiplexed recording, make it an attractive new measurement tool that will extend substantially the scope of fundamental and applied electrophysiology studies to regimes hard to access by current methods.

Methods

Silicon nanowires were synthesized using gold-nanocluster-catalysed vapour–liquid–solid (VLS) growth as described previously[16]. After dispersing silicon

nanowires on the Si_3N_4 surface of silicon wafers, gold nanodots were defined on the top surfaces of the nanowires by electron-beam lithography and metal evaporation, and germanium nanowire branches were grown from these nanodots by another gold-catalysed VLS step. Source and drain metal contacts were defined by electron-beam lithography and metal evaporation on each side of selected germanium nanowire branches on the corresponding silicon nanowire backbones, and then a conformal and uniform SiO_2 layer was deposited on the entire chip by ALD. Photoresist was spin-coated with a thickness smaller than the height of the selected germanium nanowire branches, and buffered hydrofluoric acid was then used to remove the SiO_2 from the exposed tips of the germanium–SiO_2 core–shell structure. Following photoresist lift-off, H_2O_2 was used to etch the germanium nanowire cores and yield the final BIT-FET devices. Conductance versus V_{wg} measurements were carried out in ×1 PBS buffer using an Ag/AgCl electrode. Electrical recordings from embryonic chicken cardiomyocytes were carried out using methods published previously[10,16], with cells cultured on thin PDMS films and device chips modified with lipid layers. A glass micropipette was used to control the relative position of the cell and the nanotube(s) of the BIT-FET device(s), and Ag/AgCl reference electrodes were used to fix the extracellular solution potential. The BIT-FET bandwidth as a function of nanotube inner diameter was determined from simulations of the time-dependent change in potential at the silicon-nanowire FET surface, V_n, following a potential step change at the open nanotube end.

Received 14 October 2011; accepted 16 November 2011; published online 18 December 2011

References

1. Sakmann, B. & Neher, E. Patch clamp techniques for studying ionic channels in excitable membranes. *Annu. Rev. Physiol.* **46,** 455–472 (1984).
2. Molleman, A. *Patch Clamping: An Introductory Guide to Patch Clamp Electrophysiology* (Wiley, 2003).
3. Rutten, W. L. C. Selective electrical interfaces with the nervous system. *Annu. Rev. Biomed. Engl.* **4,** 407–452 (2002).
4. Purves, R. D. *Microelectrode Methods for Intracellular Recording and Ionophoresis* (Academic Press, 1981).
5. Chorev, E., Epsztein, J., Houweling, A. R., Lee, A. K. & Brecht, M. Electrophysiological recordings from behaving animals—going beyond spikes. *Curr. Opin. Neurobiol.* **19,** 513–519 (2009).
6. Dunlop, J., Bowlby, M., Peri, R., Vasilyev, D. & Arias, R. High-throughput electrophysiology: an emerging paradigm for ion-channel screening and physiology. *Nature Rev. Drug Discov.* **7,** 358–368 (2008).
7. Hai, A., Shappir, J. & Spira, M. E. In-cell recordings by extracellular microelectrodes. *Nature Methods* **7,** 200–202 (2010).
8. Schrlau, M. G., Dun, N. J. & Bau, H. H. Cell electrophysiology with carbon nanopipettes. *ACS Nano* **3,** 563–568 (2009).
9. De Asis, E. D., Leung, J., Wood, S. & Nguyen, C. V. High spatial resolution single multiwalled carbon nanotube electrode for stimulation, recording, and whole cell voltage clamping of electrically active cells. *Appl. Phys. Lett.* **95,** 153701 (2009).
10. Tian, B. *et al.* Three-dimensional, flexible nanoscale field-effect transistors as localized bioprobes. *Science* **329,** 831–834 (2010).
11. Sze, S. M. & Ng, K. K. *Physics of Semiconductor Devices* 3rd edn (Wiley Interscience, 2006).
12. Patolsky, F., Zheng, G. & Lieber, C. M. Nanowire-based biosensors. *Anal. Chem.* **78,** 4260–4269 (2006).
13. Jiang, X. *et al.* Rational growth of branched nanowire heterostructures with synthetically-encoded properties and function. *Proc. Natl Acad. Sci. USA* **108,** 12212–12216 (2011).
14. Hausmann, D., Becker, J., Wang, S. & Gordon, R. G. Rapid vapor deposition of highly conformal silica nanolaminates. *Science* **298,** 402–406 (2002).
15. Sadiku, M. N. O. *Elements of Electromagnetics* 3rd edn (Oxford Univ. Press, 2000).
16. Cohen-Karni, T., Timko, B. P., Weiss, L. E. & Lieber, C. M. Flexible electrical recording from cells using nanowire transistor arrays. *Proc. Natl Acad. Sci. USA* **106,** 7309–7313 (2009).
17. Scanziani, M. & Hausser, M. Electrophysiology in the age of light. *Nature* **461,** 930–939 (2009).
18. Davie, J. T. *et al.* Dendritic patch-clamp recording. *Nature Protoc.* **1,** 1235–1247 (2006).
19. Bers, D. M. Cardiac excitation–contraction coupling. *Nature* **415,** 198–205 (2002).
20. Zipes, D. P. & Jalife, J. *Cardiac Electrophysiology: From Cell to Bedside* 5th edn (Saunders, 2009).
21. Buck, R. P. & Grabbe, E. S. Electrostatic and thermodynamic analysis of suspension effect potentiometry. *Anal. Chem.* **58,** 1938–1941 (1986).
22. Tasaki, I. & Singer, I. Some problems involved in electric measurements of biological systems. *Ann. NY Acad. Sci.* **148,** 36–53 (1968).
23. Chernomordik, L. V. & Kozlov, M. M. Mechanics of membrane fusion. *Nature Struct. Mol. Biol.* **15,** 675–683 (2008).
24. Almquist, B. D. & Melosh, N. A. Fusion of biomimetic stealth probes into lipid bilayer cores. *Proc. Natl Acad. Sci. USA* **107,** 5815–5820 (2010).
25. Yan, H. *et al.* Programmable nanowire circuits for nanoprocessors. *Nature* **470,** 240–244 (2011).
26. International Technology Roadmap for Semiconductors (2009); available online at http://www.itrs.net.

Acknowledgements

The authors thank Z. Jiang and H. Yan for helpful discussions. R.G. acknowledges a Japan Student Services Organization Graduate Research Fellowship. C.M.L. acknowledges a NIH Director's Pioneer Award (5DP1OD003900).

Author contributions

X.D. and C.M.L. designed the experiments. X.D., R.G., T.C-K., Q.Q., H.S.C. and B.T. performed experiments. X.D., P.X. and Q.Q. performed modelling and analyses. X.D., P.X., Q.Q., X.J. and C.M.L. analysed data. X.D., P.X. and C.M.L. wrote the paper. All authors discussed the results and commented on the manuscript.

Additional information

The authors declare no competing financial interests. Supplementary information accompanies this paper at www.nature.com/naturenanotechnology. Reprints and permission information is available online at http://www.nature.com/reprints. Correspondence and requests for materials should be addressed to C.M.L.